

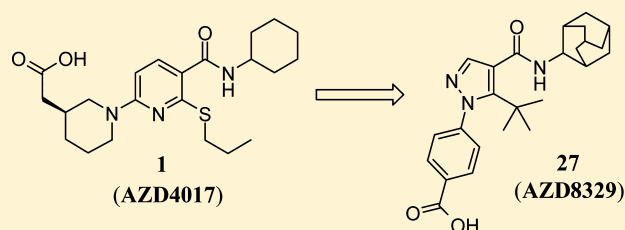
Novel Acidic 11β -Hydroxysteroid Dehydrogenase Type 1 (11β -HSD1) Inhibitor with Reduced Acyl Glucuronide Liability: The Discovery of 4-[4-(2-Adamantylcarbamoyl)-5-*tert*-butyl-pyrazol-1-yl]benzoic Acid (AZD8329)

James S. Scott,* Joanne deSchoolmeester, Elaine Kilgour, Rachel M. Mayers, Martin J. Packer, David Hargreaves, Stefan Gerhardt, Derek J. Ogg, Amanda Rees, Nidhal Selmi, Andrew Stocker, John G. Swales, and Paul R. O. Whittamore

Cardiovascular & Gastrointestinal Innovative Medicines Unit, AstraZeneca Mereside, Alderley Park, Macclesfield, Cheshire, SK10 4TG, United Kingdom

S Supporting Information

ABSTRACT: Inhibition of 11β -HSD1 is viewed as a potential target for the treatment of obesity and other elements of the metabolic syndrome. We report here the optimization of a carboxylic acid class of inhibitors from AZD4017 (**1**) to the development candidate AZD8329 (**27**). A structural change from pyridine to pyrazole together with structural optimization led to an improved technical profile in terms of both solubility and pharmacokinetics. The extent of acyl glucuronidation was reduced through structural optimization of both the carboxylic acid and amide substituents, coupled with a reduction in lipophilicity leading to an overall increase in metabolic stability.



INTRODUCTION

The metabolic syndrome is a collection of abnormalities including resistance to insulin, obesity, dyslipidemia, hyperglycemia and hypertension that represents a major risk factor for cardiovascular disease and type II diabetes.¹ It has been proposed that elevated intracellular levels of the glucocorticoid hormone cortisol in liver and adipose tissue can lead to glucose intolerance and insulin resistance and can contribute to the development of the metabolic syndrome.^{2–4}

11β -Hydroxysteroid dehydrogenase type 1 (11β -HSD1) is an NADPH dependent reductase expressed mainly in liver, adipose and brain tissue that converts the glucocorticoid inactive hormone cortisone to the glucocorticoid active hormone cortisol.⁵ Inhibition of this enzyme has the potential to reduce intracellular glucocorticoid concentrations and has been proposed as an attractive therapeutic paradigm for treatment of the metabolic syndrome.^{6–8} The considerable interest in this target is reflected by the large number of publications and patent applications as described in recent reviews.^{9–11}

11β -Hydroxysteroid dehydrogenase type 2 (11β -HSD2) is an NAD dependent oxidase expressed mainly in kidney and colon tissue that catalyzes the reverse reaction and prevents cortisol activation of mineralocorticoid receptors.¹² Selectivity against this isoform was viewed as an essential requirement in order to avoid any risk of hypertensive effects.¹³

In a previous publication, we described the identification of compound **1** (AZD4017, Figure 1)¹⁴ as a potent and selective acidic inhibitor of 11β -HSD1. During profiling of this

compound, we had observed that the major route of elimination was formation of an acyl glucuronide metabolite. This is a normal metabolic fate for acids,^{15,16} and moreover in the case of compound **1** we had not observed any covalent binding to proteins that can be associated with adverse toxicological events. Nevertheless, as part of a back-up program, we deemed it desirable to seek to identify a candidate with a similar biological profile but with a reduced propensity to form an acyl glucuronide.

Our start point for this program of work was the pyridine amide lead **2** previously identified from a high throughput screening campaign.¹⁴ We believed that the thiopropyl substituent in combination with the amide functionality was important for binding and thus screened a diverse range of five and six membered heterocycles that contained this fragment. This led to the identification of pyrazole **3** that showed considerably enhanced potency at similar lipophilicity (Table 1). The structural change from pyridine to pyrazole resulted in an increase in both ligand lipophilicity efficiency (LLE; $\text{pIC}_{50} - \log D$)¹⁷ and ligand efficiency as measured per heavy atom count. The pyrazole retained the high free drug levels observed with the pyridine core but, in common with the pyridine **2**, pyrazole **3** showed no oral exposure when dosed in a rat pharmacokinetic study.

Received: August 30, 2012

Published: October 22, 2012

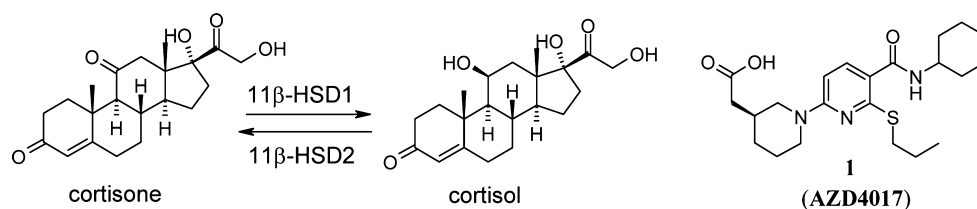


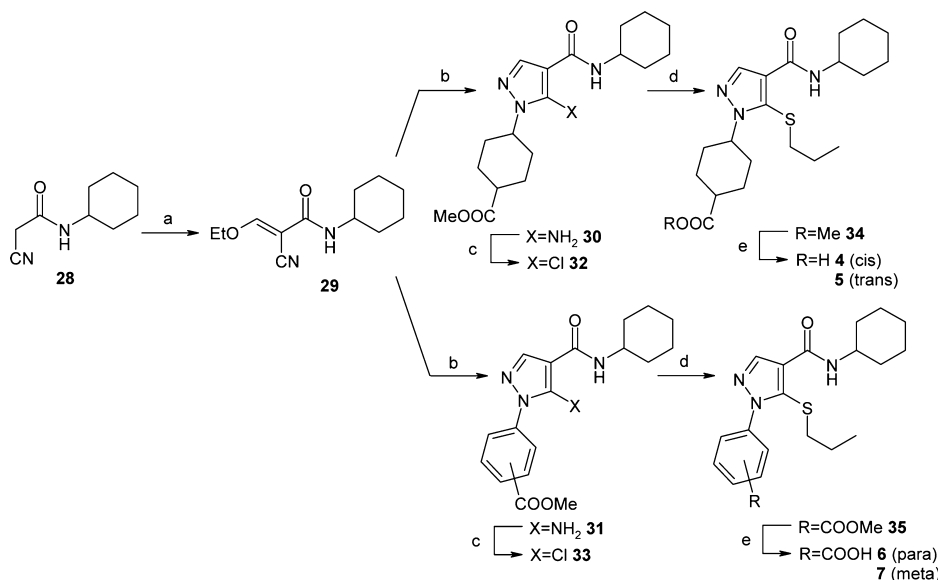
Figure 1. Interconversion of cortisone and cortisol by 11β-HSD1 and 11β-HSD2 and the acidic inhibitor AZD4017 (1).

Table 1. Enzyme Potencies, Physical and DMPK Properties for Substituted Pyrazoles

Scheme 1 shows the synthesis of pyrazoles 2 and 3. Pyrazole 2 is synthesized from 2-cyano-N-cyclohexylacetamide (28) and triethylorthoformate (29) via reaction (a). Pyrazole 3 is synthesized from 28 and 29 via reaction (b). Pyrazole 3 is further substituted with a cyclohexyl group via reaction (c) to give 30, and then with a piperidine group via reaction (d) to give 31. Pyrazole 3 is also substituted with a piperidine group via reaction (e) to give 32, and then with a piperidine group via reaction (f) to give 33.

cpd	human 11β-HSD1 IC ₅₀ (μM)	logD _{7.4}	LLE (pIC ₅₀ -logD)	LE	rat PPB (% free)	rat Heps Cl _{int} (μL/min/10 ⁶ cells)	rat Cl (mL/min/kg)	rat F (%)
2	0.350	3.2	3.3	0.46	13.0	284	41	0
3	0.018	3.0	4.7	0.55	13.2	120	21	0

Scheme 1. Synthesis of Pyrazoles 4–7^a



^a(a) (OEt)₃CH, Ac₂O, 140 °C, 5 h, 38%; (b) RNHNH₂·HCl, (iPr)₂NEt, CH(O^tBu)₂NMe₂, EtOH, 70 °C, 1 h, 32–66%; (c) ^tBuONO, CuCl₂, MeCN, 65 °C, 15 min, 30–65%; (d) ⁿPrSH, NaHMDS, DMF, 20 °C, 2 h, 65–86%; (e) NaOH, MeOH, 60 °C, 24 h, 48–98%.

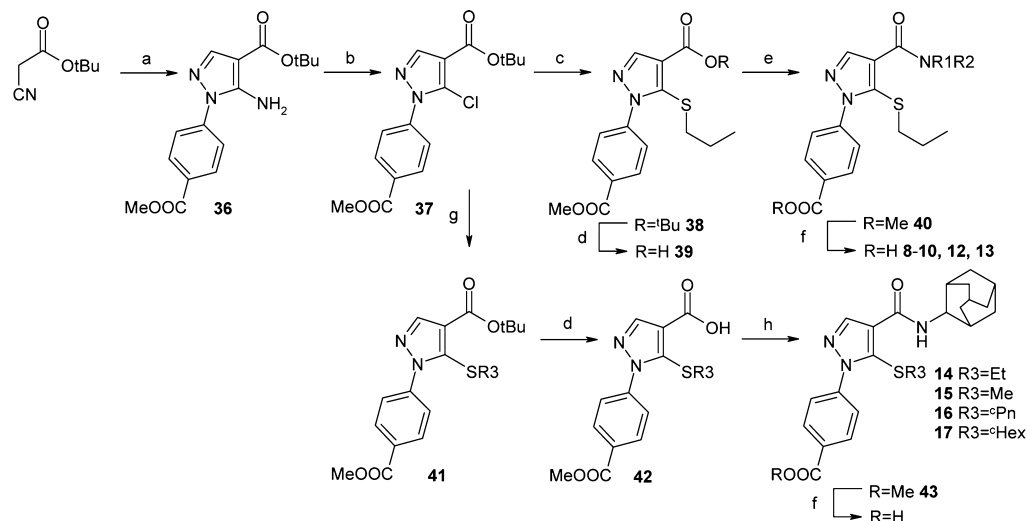
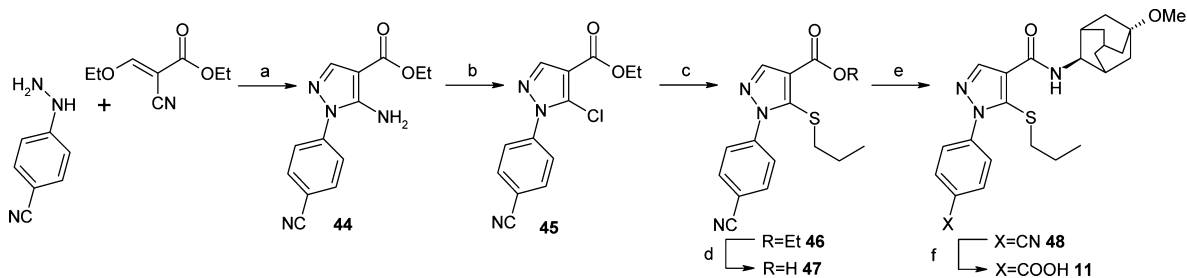
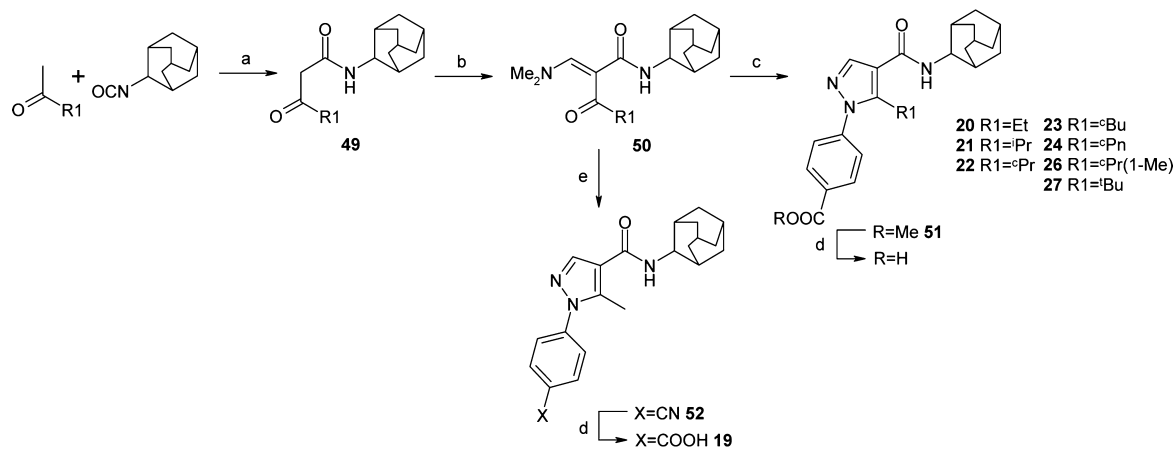
In efforts to optimize the oral exposure of pyrazole 3 we sought to introduce acidic functionality with the hope of achieving improved pharmacokinetics.¹⁴ Our initial efforts focused on substitution at the 1*N*-pyrazole position and the synthesis of compounds made as part of this optimization effort are detailed below (Schemes 1–5).

SYNTHESIS

Pyrazoles were initially constructed via a route that involved the condensation of 2-cyano-*N*-cyclohexylacetamide **28** with triethylorthoformate to give the enamide **29** (Scheme 1). Reaction with alkyl or aryl hydrazines produced the corresponding aminopyrazoles **30** and **31**. The amino functionality could be converted to chloro through diazotization with *tert*-butylnitrite followed by treatment with cupric chloride to give chloropyrazoles **32** and **33**. The chlorine was subsequently displaced with propane thiol using sodium hexamethyldisilazide as the base to

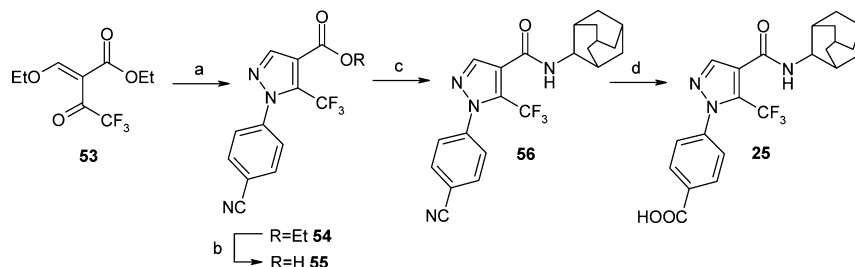
give thiopropylpyrazoles **34** and **35**. Hydrolysis of the aryl esters under basic conditions produced the pyrazole acids **4–7**.

In order to facilitate exploration of the amide functionality, the pyrazole core could also be constructed with a *tert*-butyl ester instead of an amide substituent (Scheme 2). Treatment of *tert*-butyl cyanoacetate with triethylorthoformate followed by reaction with methyl 4-hydrazinobenzoate gave the aminopyrazole **36**. Diazotisation followed by treatment with cupric chloride gave the chloropyrazole **37** which could be displaced with propylthiol to give the thiopyrazole **38**. Cleavage of the *tert*-butyl ester with trifluoroacetic acid gave the acid **39**. This could be coupled with a range of amines under HOBt/EDCI coupling conditions to give intermediates of type **40** that, after hydrolysis of the aryl ester, afforded compounds **8–10**, **12** and **13**. Treatment of chloropyrazole **37** with a range of thioalkyl groups produced thioalkylpyrazoles of type **41**. These could be converted to compounds **14–17** following a similar sequence

Scheme 2. Synthesis of Thiopyrazoles 8–10, 12–17^aScheme 3. Synthesis of Pyrazole 11^aScheme 4. Synthesis of Thiopyrazoles 19–24, 26, 27^a

of *tert*-butyl ester cleavage to **42**, amide coupling with 2-adamantylamine to **43** and aryl ester hydrolysis.

In the case of the methoxy substituted adamantyl **11**, the chemistry involved an analogous route but with 4-cyano

Scheme 5. Synthesis of Trifluoropyrazole 25^a

^aReagents: (a) (4-CN)C₆H₄NHNH₂·HCl, EtOH, 20 °C, 16 h, 77%; (b) KOSiMe₃, THF, 20 °C, 3 h, 73%; (c) 2-adamantylamine.HCl, HOBT, EDCl, (iPr)₂NEt, DMF, 20 °C, 16 h, 58%; (d) NaOH, MeOH, 65 °C, 45 h, 93%.

Table 2. Enzyme Potencies, Physical and DMPK Properties for 1*N*-Substituted Pyrazoles

Compound	R	human 11β-HSD1 IC ₅₀ (μM)	logD _{7.4}	LLE (pIC ₅₀ -logD)	Rat PPB (%free)	Rat Heps Clint (uL/min/10 ⁶ cells)	Rat Cl (mL/min/kg)	Rat F (%)
4		0.38	1.4	5.0		58	43	49
5		0.26	1.0	5.5	9.3	7.5	2.5	100
6		0.029	0.6	6.9	4.0	<3	4.5	72
7		0.16	0.7	6.1	2.0	17	17	>100

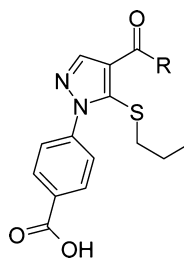
substituted hydrazine as starting material (Scheme 3). Construction of the pyrazole core **44** occurred in good yield then conversion of the amino group to a chloride **45** followed by displacement with propylthiol gave the thiopyrazole **46**. Careful optimization revealed that the ester could be selectively hydrolyzed in the presence of the nitrile using potassium trimethylsilylanolate to furnish the pyrazole acid **47**. Amide coupling with *trans*-5-methoxyadamantan-2-amine under HOBT/EDCI coupling conditions gave cyano **48** which was hydrolyzed under basic conditions to give acid **11**.

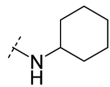
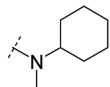
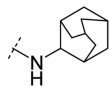
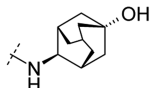
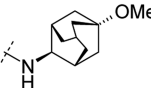
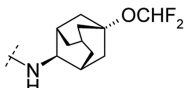
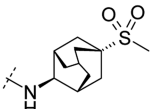
For compounds with a carbon linked substituent, routes were developed that involved addition of ketones to 2-isocyanatoadamantane to form β-keto esters of type **49** (Scheme 4). Reaction with *N,N*-dimethylformamide dimethyl acetal gave the corresponding enamines **50**. Treatment with methyl 4-

hydrazinobenzoate formed pyrazoles **51** then hydrolysis of the ester produced final compounds **20–24**, **26** and **27**. In the case of compound **19**, this was constructed in an analogous fashion but using 4-cyano phenylhydrazine to form pyrazole **52**. Hydrolysis of the cyano group gave the desired acid **19**.

Trifluoropyrazole **25** was synthesized via a route reacting ethyl 2-(ethoxymethylene)-4,4,4-trifluoro-3-oxobutanoate **53** with 4-cyano phenylhydrazine to construct the pyrazole core **54** (Scheme 5). Selective hydrolysis of the ethyl ester in the presence of the nitrile using potassium trimethylsilylanolate furnished the pyrazole acid **55**. Amide coupling with 2-adamantylamine under HOBT/EDCI coupling conditions gave cyano **56** which was hydrolyzed under basic conditions to give acid **25**.

Table 3. Enzyme Potencies, Physical and DMPK Properties for Amide Variation



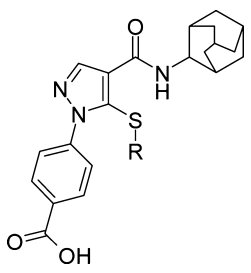
Compound	R	human 11 β -HSD1 IC ₅₀ (μ M)	logD _{7.4}	LLE (pIC ₅₀ - logD)	Rat PPB (%free)	Rat Heps Clint (uL/min/ 10 ⁶ cells)	Rat Cl (mL/min/kg)	Rat F (%)
6		0.029	0.6	6.9	4.0	<3	4.5	72
8		0.043	0.6	6.8	2.5	26	8.1	26
9		0.003	1.8	6.7	0.5	4.7	2	45
10		0.006	-0.4	8.6	10.5	<2	20	10
11		0.005	<0.5		28.5	<2	13	54
12		0.012	1.2	6.8	2.6	18	9.4	40
13		0.19	<0.5		13.4	2.6	83	7

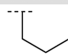
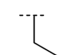
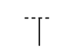
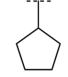
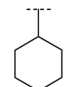
RESULTS AND DISCUSSION

Both *cis* **4** and *trans* **5** cyclohexylacids showed modest potency with the *trans* isomer **5** being slightly more potent and with a higher LLE (5.5). The introduction of acidic functionality resulted in improved oral exposure of these compounds with the *trans* isomer **5** in particular showing high stability in hepatocytes that translated into low *in vivo* clearance and complete bioavailability (100%). As both stereoisomers retained potency we felt this indicated some degree of spatial tolerance for acidic functionality. We explored alternative linking groups and as a consequence made the benzoic acids **6** and **7**. The *para*-substituted acid resulted in an increase in potency together with a lowering of lipophilicity that resulted in an increase in LLE (6.9). Compound **6** has reasonable free levels for an acid and showed low turnover in rat hepatocytes that corresponded to low *in vivo* clearance and excellent bioavailability (Table 2).

In efforts to increase potency, we investigated the SAR of the amide substituent (Table 3). In contrast to the results observed in the previous pyridine series, ¹⁴N-methylcyclohexyl amide **8** did not improve potency and led to a decrease in stability in rat hepatocytes and a reduction in oral bioavailability. 2-Adamantyl **9** increased 10-fold in potency relative to **6** but at the expense of a log unit increase in lipophilicity leading to an overall similar value for LLE (6.7). Despite this, the *in vitro* and *in vivo* clearance remained low and the compound had moderate bioavailability. Attempts to introduce a hydroxyl substituent **10** onto the adamantyl ring resulted in retention of potency despite a lowering of lipophilicity and a corresponding increase in LLE (8.6). Despite high stability in hepatocytes, the compound showed increased *in vivo* clearance and poor bioavailability, potentially as a result of high free drug levels. The corresponding methyl **11** and difluoromethyl **12** ethers retained good potency and showed improved bioavailability over the corresponding hydroxyl **10**. Sulphone **13** showed a drop in potency and very

Table 4. Enzyme Potencies, Physical and DMPK Properties for Thioalkyl Pyrazoles



Compound	R	human 11 β -HSD1 IC ₅₀ (μ M)	logD _{7.4}	LLE (pIC ₅₀ -logD)	Rat PPB (%free)	Rat Heps Clint (uL/min/10 ⁶ cells)	Rat Cl (mL/min/kg)	Rat F (%)
9		0.003	1.8	6.7	0.5	4.7	2	45
14		0.004	1.5	6.9	1.31	6	3	65
15		0.010	1.2	6.8	3.36	<2	11	64
16		0.005	2.6	5.7	0.15	14	3.3	57
17		0.011	3.0	4.9	0.13	9.4	3.6	82

high *in vivo* clearance leading to poor bioavailability for this compound.

On balance we concluded that adamantyl **9** represented the most promising point for further optimization and looked to optimize the thio-alkyl substituent (Table 4). Truncation of the thiopropyl-substituent to ethyl **14** and methyl **15** resulted in small reductions in potency and an increase in free drug levels, as expected based on the reduction in lipophilicity. Expansion to the five-membered ring **16** increased lipophilicity but did not bring a corresponding increase in potency, leading to a reduction in LLE (5.7). Further expansion to the six-membered ring **17** resulted in a further drop in potency and a lower LLE (4.9).

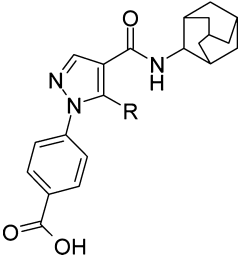
Although compound **15** looked attractive in terms of overall profile, we elected to reinvestigate the SAR with respect to whether the thio-group could be replaced (Table 5). Simple deletion of the thio-substituent (**18**) resulted in a significant loss in potency. Replacement with methyl **19** failed to increase potency but extension to ethyl **20** resulted in a significant improvement in LLE (5.5). Branching at this position, as exemplified by isopropyl **21**, resulted in a further improvement in LLE (6.6). The 3 and 4-membered cyclic variants **22** and **23** maintained similar LLE levels although this deteriorated upon expansion to the 5-membered ring **24**. Notably, cyclopropyl **22** was less stable in rat hepatocytes than either the isopropyl **21** or cyclobutyl **23** and this translated to higher *in vivo* clearance in rat. Replacement with trifluoromethyl **25** resulted in a drop in potency and a reduction in LLE. The methyl cyclopropyl **26** and *tert*-butyl **27** analogues showed a further increase in LLE (7.1 and 7.0 respectively) surpassing the thiopropyl compound **9** (LLE 6.7) in terms of efficiency. In a similar manner to **22**, cyclopropyl **26** had moderate turnover in rat hepatocytes and moderate *in vivo* clearance in rat. In contrast, *tert*-butyl **27** was significantly

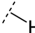
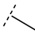
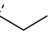
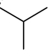

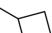
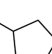
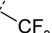


more stable both *in vitro* and *in vivo* leading to an excellent pharmacokinetic profile for this compound.

We obtained a crystal structure of compound **27** bound in the active site of 11 β -HSD1, using conditions described previously.¹⁴ Figure 2A shows the binding mode of compound **27** highlighting the key interactions of the amide carbonyl with Ser170 and of the acid which has a strong hydrogen bond contact to Tyr284. Figure 2B shows the structure of **27** overlaid with that of **1**. The cyclohexyl ring of **1** and the NH group overlay very closely with a cyclohexyl ring of the adamantane portion of compound **27**. The amide carbonyl groups are at different angles; this is accommodated by a change in position of the Ser170 side chain, which makes a contact with the carbonyl in both complexes. There is no equivalent to the propyl chain of **1**, but a methyl group from the *tert*-butyl substituent is overlaid on the sulfur atom. The acid groups occupy very different positions in the active site. In **1**, we noted a key interaction with the backbone at Leu217; this interaction is absent for compound **27** and instead we observe a strong hydrogen bond contact to Tyr284. This residue is not resolved in the structure with **1** and it appears that compound **27** is able to stabilize the C-terminal loop of the protein via this interaction, with the effect that it is now clearly visible in the electron density. Comparing the ribbon trace for the structure of **1** (yellow) with that of compound **27** (orange), we see that the loop comprising residues Gly229 to His232 is pushed outward (on the right of the Figure 2B) to accommodate the tyrosine side chain. The C-terminal loop in the AZD4017 structure is not resolved beyond Ser283.

On the basis of this program of work, compound **27** was profiled further (Table 6). The compound showed no significant activity (<25% inhibition at 10 μ M) against five isoforms of the cytochrome P450 enzymes (CYP1A2, CYP2C9, CYP2C19,

Table 5. Enzyme Potencies, Physical and DMPK Properties for Nonthioalkyl Pyrazoles



Compound	R	human 11 β -HSD1 IC ₅₀ (μ M)	logD _{7.4}	LLE (pIC ₅₀ -logD)	Rat PPB (%free)	Rat Heps Clint (uL/min/10 ⁶ cells)	Rat Cl (mL/min/kg)	Rat F (%)
18		2.3			10.7	6.6		
19		7.6	0.8	4.3	12.7	<3	8	>100
20		0.38	0.9	5.5	6.0	<2	7.3	>100
21		0.017	1.2	6.6	3.6	<2	2.2	53
22		0.021	0.9	6.8	4.5	15	14	51
23		0.010	1.3	6.7	1.2	<3	1.3	>100
24		0.009	1.7	6.3	0.4	<2	0.6	>100
25		0.11	1.5	5.5	4.5	<3	3.8	>100
26		0.006	1.1	7.1	3.3	11	19	>100
27		0.009	1.0	7.0	1.3	<2	0.6	95

CYP2D6 and CYP3A4). Plasma protein binding showed good free levels for an acid (1.3–3.5% free across species) in line with the low lipophilicity of the compound (logD_{7.4} 1.0). The measured pK_A of the carboxylic acid was 3.9. The solubility as measured on crystalline material was >1900 μ M and when taken together with moderate cellular permeability, as measured in an MDCK assay (P_{app}(A-B) 7.3 $\times 10^{-6}$ cm.s⁻¹; efflux ratio 0.5), it was predicted that this would lead to good absorption *in vivo*. Four stable, nonsolvated crystalline forms were identified and no photostability issues or chemical stability concerns across the pH range 1–10 were highlighted with this compound.

The pharmacokinetic profile of compound 27 was examined in other species and the results are summarized in Table 7. The compound showed good properties (mouse, rat, dog) with low *in vivo* clearance in mouse and very low *in vivo* clearance in both rat and dog. Volumes of distribution were low as expected of an acidic compound and good bioavailabilities (F > 40%) were observed across all three species. The renal component of the

in vivo clearance was found to be minimal, comprising <1% of the total clearance in rat and <5% in dog. Compound 27 tested negative for reactive metabolites from oxidative metabolism in an *in vitro* trapping assay in human liver microsomes using reduced glutathione as a trapping agent.

In order to understand the mechanism of clearance, compounds 1 and 27 were incubated in hepatocytes and the proportion of glucuronidation relative to oxidative metabolism, as measured by peak area of metabolites, was calculated as shown in Table 8. In the case of compound 1, acyl glucuronidation was the predominant metabolic pathway for this compound in all three species with ratios relative to oxidative metabolism of approximately 2, 4, and 6 in rat, dog and human respectively. In stark contrast, compound 27 showed significantly greater metabolic stability (greater % parent remaining) and minimal amounts of acyl glucuronide formation (0.5% or less) in all three species. A switch to oxidative metabolism as the predominant metabolic pathway had occurred such that the ratios of acyl

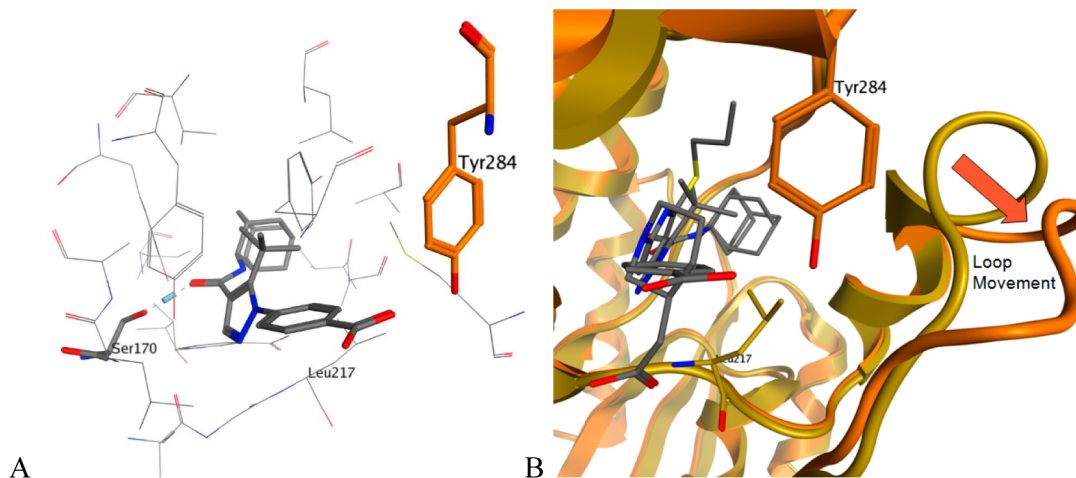


Figure 2. (A) Crystal structure of compound 27 bound to human 11 β -HSD1 highlighting key residues Ser170 and Tyr284. (B) Crystal structure of compound 27 bound to human 11 β -HSD1, overlaid with 1. The protein constructs are identical, but compound 27 induces a loop motion, as seen to the right, due to ordering of Tyr284 via a strong hydrogen bond contact.

Table 6. Physical Properties of Compound 27

aqueous solubility ^a (μM)	mouse PPB ^b (% free)	rat PPB ^b (% free)	dog PPB ^b (% free)	human PPB ^b (% free)	MDCK ^c permeability Papp ($\times 10^{-6} \text{ cm s}^{-1}$)
>1900 ($n = 2$)	3.5 ($n = 1$)	1.3 ($n = 3$)	2.0 ($n = 2$)	1.4 ($n = 2$)	7.3 (A-B); 3.9 (B-A) ($n = 3$)

^aSolubility of compounds in aqueous phosphate buffer at pH 7.4 after 24 h at 25 °C (μM). ^bPPB was assessed by equilibrium dialysis in the appropriate species plasma at 37 °C. Free and bound concentrations were quantified by LC-UVMS. ^cCompounds were incubated at 10 μM in cultured MDCK cells. Permeability was measured in both the A to B and B to A direction.

Table 7. Pharmacokinetic Parameters for Selected Compound 27^a

species	Cl _p (mL/min/kg)	V _{d,ss} (L/kg)	i.v. half-life (h)	oral half-life (h)	bioavailability (%)
mouse	9	0.4	0.8	2.2	100
rat	0.6	0.3	5.8	4.9	95
dog	0.3	0.1	5.5	5.1	45

^aDosed at between 1 and 3 mg/kg in either solution (DMSO/hydroxy-beta-cyclodextrin) or suspension (HPMC/Tween).

Table 8. Metabolism-ID Summaries for Selected Compounds 1 and 27

cpd	species	parent (%)	[+Glu] (%)	[+O] (%)	ratio [+Glu]:[O]
1	rat	66	23	11	2.1
1	dog	34	53	13	4.1
1	human	93	6	1	6
27	rat	96	0.1	3.9	0.02
27	dog	93.7	0.5	5.8	0.08
27	human	95	0.4	4.6	0.10

glucuronidation to oxidative metabolism were now 0.1 or less. We rationalized these observations as being a combination of several factors; in the nature of the carboxylic acid (aryl vs alkyl) dis-favoring acyl glucuronidation; the higher local lipophilicity of the amide (adamantyl vs cyclohexyl) favoring metabolism; and the overall reduction in lipophilicity leading to an overall increase in metabolic stability.

A metabolism-ID study was carried out in bile duct cannulated rats with the results for the 0–6 h samples shown in Table 9. For

Table 9. Metabolism-ID Summaries in Rat Bile and Urine for Selected Compounds 1 and 27

cpd	excreta	parent (%)	[+Glu] (%)	[+O] (%)	ratio [+Glu]:[O]
1	rat bile	15	75	10	7.5
1	rat urine	4	68	28	2.4
27	rat bile	10.8	9.1	80.1	0.1
27	rat urine	99.4	0.4	0.2	2.0

compound 1, acyl glucuronidation was the predominant metabolic pathway. By contrast, oxidation was the main route of metabolism observed for compound 27 in rat bile, with lower amounts of glucuronide detected (9% vs 75% for 1). In rat urine, the majority of the analyte was parent (99.4%), with only low levels of the glucuronide (0.4%) and oxidized products (0.2%) being detected, consistent with the lower clearance of this compound. Three isomers of the glucuronide of 27 were detected in rat bile compared to five glucuronide isomers of compound 1.

Compound 27 displayed excellent selectivity versus the related enzymes 11 β -HSD2 ($\text{IC}_{50} > 30 \mu\text{M}$), 17 β -HSD1 ($\text{IC}_{50} > 30 \mu\text{M}$) and 17 β -HSD3 (<5% inhibition at 10 μM) and showed no measurable activity against the glucocorticoid or mineralocorticoid receptors. Further profiling revealed that compound 27 was nonmutagenic in a two-strain Ames test and negative in a mouse lymphoma assay. It had an $\text{IC}_{50} > 100 \mu\text{M}$ in the hERG IonWorks assay and was assessed in a guinea pig MAP assay with no changes observed in any parameters. A good selectivity profile (>2500 fold selective) was observed versus a diverse panel of 140 targets.

Profiling of 11- β HSD1 activity across species revealed that, although the potency of compound 27 was similar to that of 1 in human and cynomolgous monkey, significant improvements were observed in the rat (>50 fold) and dog (>450 fold) activity. The potency as measured in human adipocytes ($\text{IC}_{50} 0.002 \mu\text{M}$) was in good agreement with the enzyme potency (Table 10).

Because of the improved potency of 27 in rat relative to 1 it was feasible to carry out pharmacodynamic measurements in an ex vivo assay measuring the inhibition of conversion of ³H-cortisone

Table 10. In Vitro Potencies for Compounds 1 and 27

cpd	human enzyme IC ₅₀ (μM)	mouse enzyme IC ₅₀ (μM)	rat enzyme IC ₅₀ (μM)	dog enzyme IC ₅₀ (μM)	cyno enzyme IC ₅₀ (μM)	human adipocyte IC ₅₀ (μM)
1	0.007	0.750	4.06	3.77	0.029	0.002
27	0.009	6.1	0.086	0.008	0.024	0.002

to ³H-cortisol in this preclinical species. The effects in adipose and liver tissue of dosing compound 27 orally to lean rats (1–30 mg/kg) are shown in Figure 3. At 3 h post dose at 3 mg/kg, 50%

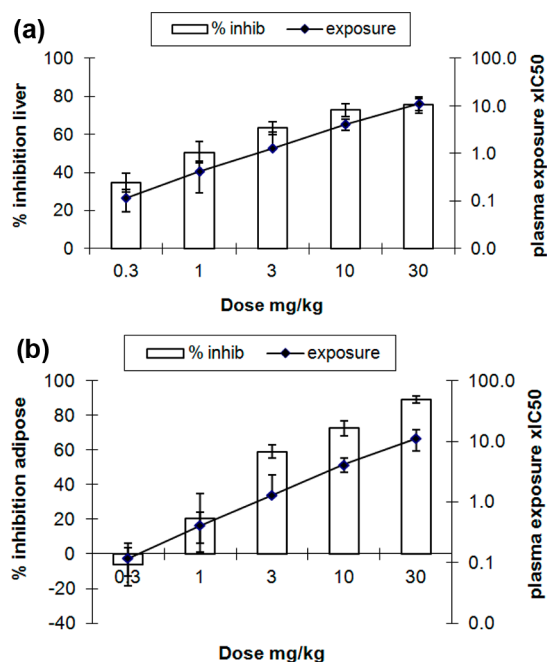


Figure 3. Inhibition of 11β-HSD1 in mouse ex vivo model in adipose and liver for compound 27.

inhibition was observed in liver tissue, approximately equal to the in vitro rat IC₅₀. In adipose tissue, a similar observation was made at a dose of 10 mg/kg, approximating to five times the rat IC₅₀ value.

In summary, we have discovered novel acidic inhibitors of 11β-HSD1 that show excellent physicochemical and pharmacokinetic profiles. Re-engineering of the initial structure involving a structural change from pyridine to pyrazole, a switch from an alkyl to an aryl acid and replacement of a thioalkyl group with a *tert*-butyl substituent resulted in compound 27 that had significantly reduced acyl glucuronidation liability. On the basis of a strong technical profile and the ability to inhibit 11β-HSD1 in both rat liver and adipose tissue, compound 27 was selected for development as AZD8329 and progressed into toxicity studies. The results of further studies with this compound will be reported in due course.

EXPERIMENTAL SECTION

All solvents and chemicals used were reagent grade. Anhydrous solvents tetrahydrofuran (THF), dimethylformamide (DMF) and dimethylacetamide (DMA) were purchased from Aldrich. Flash column chromatography was carried out using prepacked silica cartridges (from 4 g up to 330 g) from Rediseq, Biotage or Crawford and eluted using an Isco Companion system. ¹H NMR were recorded on a Varian Gemini 2000 (300 MHz) or a Bruker Avance DPX400 (400 MHz) and were determined in CDCl₃ or DMSO-*d*₆. Chemical shifts are reported in

ppm relative to tetramethylsilane (TMS) (0.00 ppm) or solvent peaks as the internal reference and coupling constant (*J*) values are reported in Hertz (Hz). Splitting patterns are indicated as follows: s, singlet; d, doublet; t, triplet; m, multiplet; br, broad peak. Merck precoated thin layer chromatography (TLC) plates (silica gel 60 F₂₅₄, 0.25 mm, art. 5715) were used for TLC analysis. The purity of compounds submitted for screening was >95% as determined by UV analysis of liquid chromatography–mass spectroscopy (LC–MS) chromatograms at 254 nM and substantiated using the TAC (Total Absorption Chromatogram). Further support for the purity statement was provided using the MS TIC (Total Ion Current) trace in ESI +ve and –ve ion modes, HRMS and NMR analysis. Solutions were dried over anhydrous magnesium sulfate and the solvent was removed by rotary evaporation under reduced pressure.

cis-4-[4-(Cyclohexylcarbamoyl)-5-propylsulfanyl-pyrazol-1-yl]cyclohexanecarboxylic Acid (4). *cis*-Ethyl 4-[4-(cyclohexylcarbamoyl)-5-propylsulfanyl-pyrazol-1-yl]cyclohexane-1-carboxylate 34a (116 mg, 0.28 mmol) was dissolved in methanol (5 mL) and treated with 2 M sodium hydroxide (1.4 mL, 2.80 mmol). The mixture was stirred at ambient temperature for 24 h. The reaction mixture was concentrated in vacuo to remove the methanol and diluted with water (25 mL). The aqueous solution was washed with ether (20 mL), acidified to pH 3 with 2 M HCl and extracted with EtOAc (3 × 25 mL). The combined extracts were washed with water (2 × 20 mL) and brine (10 mL), dried (MgSO₄) and evaporated to leave a white solid. Trituration with ether gave a white solid (52 mg, 48%); ¹H NMR (400 MHz, DMSO-*d*₆) δ 0.91 (3H, t, *J* = 7.3 Hz), 1.10–1.47 (7H, m), 1.52–1.74 (7H, m), 1.77–1.84 (2H, m), 1.85–1.99 (2H, m), 2.10–2.22 (2H, m), 2.59–2.66 (1H, m), 2.87 (2H, t, *J* = 7.2 Hz), 3.66–3.79 (1H, m), 4.61–4.72 (1H, m), 7.77 (1H, d, *J* = 8.0 Hz), 7.92 (1H, s), 12.32 (1H, s); HRMS (EI) for C₂₀H₃₂O₃N₃S (MH⁺); calcd, 394.2159; found, 394.2158.

4-[4-(*N*-Cyclohexyl-*N*-methyl-carbamoyl)-5-propylsulfanyl-pyrazol-1-yl]benzoic Acid (8). Methyl 4-[4-(cyclohexyl-methyl-carbamoyl)-5-propylsulfanyl-pyrazol-1-yl]benzoate 40a (162 mg, 0.39 mmol) was dissolved in methanol (10 mL) and treated at ambient temperature with 2 M aqueous sodium hydroxide solution (0.96 mL, 1.95 mmol). The mixture was stirred at ambient temperature for 18 h. Methanol was removed by evaporation under reduced pressure and the clear solution was diluted with water (25 mL). 2 M HCl was added until pH 4 and the mixture was extracted with ethyl acetate (2 × 25 mL). The combined extracts were washed with water (2 × 10 mL) and brine (10 mL), dried (MgSO₄) and evaporated to give the title compound as a white solid (150 mg, 96%); ¹H NMR (300 MHz, DMSO-*d*₆) δ 0.68 (3H, t, *J* = 7.3 Hz), 1.10–1.41 (4H, m), 1.42–1.85 (8H, m), 2.58 (2H, t, *J* = 7.0 Hz), 2.86 (3H, s), 3.45–3.60 (0.5H, m), 4.21–4.38 (0.5H, m), 7.74 (2H, d, *J* = 8.2 Hz), 7.89 (1H, s), 8.09 (2H, d, *J* = 8.4 Hz), 13.20 (1H, s); HRMS (EI) for C₂₁H₂₈O₃N₃S (MH⁺); calcd, 402.1846; found, 402.1844.

4-[4-(2-Adamantylcarbamoyl)-5-propylsulfanyl-pyrazol-1-yl]benzoic Acid (9). Prepared according to the procedure of 8 from methyl 4-[4-(2-adamantylcarbamoyl)-5-propylsulfanyl-pyrazol-1-yl]benzoate 40b in 94% yield; ¹H NMR (300 MHz, DMSO-*d*₆) δ 0.65 (3H, t, *J* = 7.3 Hz), 1.17–1.29 (2H, m), 1.54–1.66 (2H, m), 1.68–2.06 (12H, m), 2.62 (2H, t, *J* = 7.0 Hz), 4.05–4.14 (1H, m), 7.75 (2H, d, *J* = 8.5 Hz), 8.03 (1H, d, *J* = 7.5 Hz), 8.13 (2H, d, *J* = 8.5 Hz), 8.20 (1H, s), 13.19 (1H, s); HRMS (EI) for C₂₄H₃₀O₃N₃S (MH⁺); calcd, 440.2002; found, 440.2002.

4-[4-[(*trans*)-5-Methoxy-2-adamantyl]carbamoyl]-5-propylsulfanyl-pyrazol-1-yl]benzoic Acid (11). A solution of sodium hydroxide (1.05 mL, 2.11 mmol) was added in one portion to a stirred suspension of 1-(4-cyanophenyl)-*N*-(5-methoxy-2-adamantyl)-5-propylsulfanyl-pyrazole-4-carboxamide 48 (190 mg, 0.42 mmol), in MeOH (4 mL) warmed to 60 °C. The resulting solution was stirred at 60 °C for 16 h. The reaction mixture was concentrated and diluted with 1,4-dioxane (6 mL), and a further 2 mL sodium hydroxide solution and 3 mL water were added then stirred at 100 °C for 16 h. The reaction mixture was evaporated to remove the organic solvents, and washed with CH₂Cl₂ (10 mL), the aqueous layer was acidified with 2 N HCl, and the precipitate was collected by filtration, washed with water (10 mL) and

dried under vacuum to afford a cream solid that was purified by preparative HPLC (Phenomenex Gemini C18 110A (axia) column, 5 μ m silica, 30 mm diameter, 100 mm length), using decreasingly polar mixtures of water (containing 0.5% NH₃) and MeCN as eluents. Fractions containing the desired compound were evaporated to dryness to afford a white solid (82 mg, 41%). ¹H NMR (400 MHz, DMSO-*d*₆) δ 0.66 (3H, t, *J* = 7.3 Hz), 1.18–1.30 (2H, m), 1.41–1.51 (2H, m), 1.66–1.86 (6H, m), 1.88–1.98 (2H, m), 2.07–2.18 (3H, m), 2.63 (2H, t, *J* = 7.1 Hz), 3.14 (3H, s), 3.96–4.10 (1H, m), 7.71–7.77 (1H, m), 8.01 (1H, d, *J* = 7.3 Hz), 8.08–8.15 (1H, m), 8.18 (1H, s), 13.26 (1H, s); HRMS (EI) for C₂₅H₃₂O₄N₃S (MH⁺); calcd, 470.2108; found, 470.2108.

4-[4-(2-Adamantylcarbamoyl)pyrazol-1-yl]benzoic Acid (18). Prepared according to the procedure of **8** from methyl 4-[4-(2-adamantylcarbamoyl)pyrazol-1-yl]benzoate in 28% yield; ¹H NMR (300 MHz, DMSO-*d*₆) δ 1.48–1.61 (2H, m), 1.66–1.89 (8H, m), 1.90–1.99 (2H, m), 2.04–2.18 (2H, m), 4.01–4.06 (1H, m), 7.58 (1H, d, *J* = 7.0 Hz), 7.98 (2H, d, *J* = 8.6 Hz), 8.08 (2H, d, *J* = 8.6 Hz), 8.23 (1H, s), 9.17 (1H, s), 13.00 (1H, s); HRMS (EI) for C₂₁H₂₄O₃N₃ (MH⁺); calcd, 366.1812; found, 366.1812.

4-[4-(2-Adamantylcarbamoyl)-5-methyl-pyrazol-1-yl]-benzoic Acid (19). A solution of 1 M sodium hydroxide (24.28 mL, 24.28 mmol) was added to a stirred suspension of *N*-(2-adamantyl)-1-(4-cyanophenyl)-5-methyl-pyrazole-4-carboxamide **52** (1.25 g, 3.47 mmol) in dioxane (25 mL). The resulting suspension was stirred at 100 °C for 7 h. The reaction mixture was concentrated, diluted with water (40 mL) and filtered through Celite. The filtrates were acidified with 1 M citric acid. The precipitate was recovered by filtration, washed with water (3 \times 20 mL) and dried under vacuum at 50 °C. The crude product was purified by preparative HPLC (Phenomenex Gemini C18 110A (axia) column, 5 μ m silica, 30 mm diameter, 100 mm length), using decreasingly polar mixtures of water (containing 1% formic acid) and MeCN as eluents. Fractions containing the desired compound were evaporated to dryness to afford a pale yellow powder (550 mg, 42%); ¹H NMR (400 MHz, DMSO-*d*₆) δ 1.45–1.54 (2H, m), 1.70–1.88 (8H, m), 1.90–2.00 (2H, m), 2.05–2.18 (2H, m), 2.56 (3H, s), 4.00–4.10 (1H, m), 7.55 (1H, d, *J* = 6.8 Hz), 7.63–7.68 (2H, m), 8.05–8.10 (2H, m), 8.29 (1H, s), 13.25 (1H, s); HRMS (EI) for C₂₂H₂₆O₃N₃ (MH⁺); calcd, 380.1969; found, 380.1969.

4-[4-(2-Adamantylcarbamoyl)-5-ethylpyrazol-1-yl]benzoic Acid (20). Prepared according to the procedure of **8** from methyl 4-[4-(2-adamantylcarbamoyl)-5-ethylpyrazol-1-yl]benzoate **51c** in 59% yield; ¹H NMR (400 MHz, DMSO-*d*₆) δ 1.03 (3H, t, *J* = 7.4 Hz), 1.46–1.57 (2H, m), 1.66–1.87 (8H, m), 1.90–1.98 (2H, s), 2.04–2.14 (2H, m), 2.97 (2H, q, *J* = 7.4 Hz), 3.99–4.06 (1H, m), 7.58–7.63 (3H, m), 8.09–8.13 (2H, m), 8.28 (1H, s); HRMS (EI) for C₂₃H₂₈O₃N₃ (MH⁺); calcd, 394.2125; found, 394.2124.

4-[4-(2-Adamantylcarbamoyl)-5-propan-2-ylpyrazol-1-yl]-benzoic Acid (21). Prepared according to the procedure of **8** from methyl 4-[4-(2-adamantylcarbamoyl)-5-propan-2-ylpyrazol-1-yl]benzoate **51d** in 100% yield; ¹H NMR (400 MHz, DMSO-*d*₆) δ 1.29 (6H, d, *J* = 7.0 Hz), 1.46–1.56 (2H, m), 1.66–1.88 (8H, m), 1.92–1.99 (2H, m), 2.04–2.14 (2H, m), 3.12 (1H, hept, *J* = 7.0 Hz), 4.02–4.05 (1H, m), 7.50–7.55 (2H, m), 7.67 (1H, d, *J* = 6.8 Hz), 8.05 (1H, s), 8.07–8.12 (2H, m), 13.20 (1H, s); HRMS (EI) for C₂₄H₃₀O₃N₃ (MH⁺); calcd, 408.2281; found, 408.2281.

4-[4-(2-Adamantylcarbamoyl)-5-cyclopropyl-pyrazol-1-yl]-benzoic Acid (22). Prepared according to the procedure of **8** from methyl 4-[4-(2-adamantylcarbamoyl)-5-cyclopropylpyrazol-1-yl]benzoate **51e** in 95% yield; ¹H NMR (300 MHz, DMSO-*d*₆) δ 0.41–0.46 (2H, m), 0.85–0.91 (2H, m), 1.48–1.60 (2H, m), 1.67–1.89 (8H, m), 1.90–1.99 (2H, m), 2.00–2.11 (2H, m), 2.21–2.30 (1H, m), 4.00–4.09 (1H, m), 7.58 (1H, d, *J* = 7.3 Hz), 7.77 (2H, d, *J* = 8.5 Hz), 7.94 (1H, s), 8.09 (2H, d, *J* = 8.5 Hz), 13.11 (1H, s); HRMS (EI) for C₂₄H₂₈O₃N₃ (MH⁺); calcd, 406.2125; found, 406.2123.

4-[4-(2-Adamantylcarbamoyl)-5-cyclobutylpyrazol-1-yl]-benzoic Acid (23). Prepared according to the procedure of **8** from methyl 4-[4-(2-adamantylcarbamoyl)-5-cyclobutylpyrazol-1-yl]benzoate **51f** in 99% yield; ¹H NMR (400 MHz, DMSO-*d*₆) δ 1.47–1.58 (2H, m), 1.60–1.89 (10H, m), 1.92–2.00 (2H, m), 2.03–2.13 (4H, m), 2.20–2.28 (2H, m), 3.76–3.85 (1H, m), 4.01–4.06 (1H, m), 7.48–

7.55 (2H, m), 7.80 (1H, d, *J* = 7.1 Hz), 7.93 (1H, s), 8.04–8.10 (2H, m), 13.40 (1H, s); HRMS (EI) for C₂₅H₃₀O₃N₃ (MH⁺); calcd, 406.2125; found, 406.2123.

4-[4-(2-Adamantylcarbamoyl)-5-cyclopentyl-pyrazol-1-yl]-benzoic Acid (24). Prepared according to the procedure of **8** from methyl 4-[4-(2-adamantylcarbamoyl)-5-cyclopentyl-pyrazol-1-yl]benzoate **51g** in 97% yield; ¹H NMR (400 MHz, DMSO-*d*₆) δ 1.43–1.55 (4H, m), 1.74–1.85 (12H, m), 1.89–1.96 (2H, m), 2.03–2.12 (4H, m), 2.99–3.08 (1H, m), 3.98–4.03 (1H, m), 7.53–7.55 (2H, m), 7.74 (1H, d, *J* = 6.9 Hz), 8.09 (1H, s), 8.10–8.12 (2H, m), 13.30 (1H, s); HRMS (EI) for C₂₆H₃₂O₃N₃ (MH⁺); calcd, 434.2438; found, 434.2438.

4-[4-(Adamantan-2-ylcarbamoyl)-5-(trifluoromethyl)-1H-pyrazol-1-yl]benzoic Acid (25). A solution of sodium hydroxide (1.056 mL, 2.11 mmol) was added in one portion to a stirred solution of *N*-adamantan-2-yl-1-(4-cyanophenyl)-5-(trifluoromethyl)-1H-pyrazole-4-carboxamide **56** (250 mg, 0.60 mmol), in methanol (10 mL) under air. The resulting solution was stirred at 65 °C for 45 h. The resulting mixture was evaporated to dryness and the residue dissolved in ice/water (25 mL) and the mixture was acidified with 2 M HCl. The precipitate was collected by filtration, washed with water (25 mL) and dried under vacuum to afford a white solid (243 mg, 93%). ¹H NMR (400 MHz, DMSO-*d*₆) δ 1.46–1.56 (2H, m), 1.66–1.73 (2H, m), 1.75–1.88 (5H, m), 1.89–1.97 (3H, m), 2.00–2.10 (2H, m), 3.98–4.05 (1H, m), 7.63 (2H, d, *J* = 8.5 Hz), 8.11–8.14 (3H, m), 8.34 (1H, d, *J* = 7.1 Hz), 13.30 (1H, s); HRMS (EI) for C₂₂H₂₃O₃N₃F₃ (MH⁺); calcd, 434.1686; found, 434.1684.

4-[4-(2-Adamantylcarbamoyl)-5-(1-methylcyclopropyl)-pyrazol-1-yl]benzoic Acid (26). Prepared according to the procedure of **8** from methyl 4-[4-(2-adamantylcarbamoyl)-5-(1-methylcyclopropyl)pyrazol-1-yl]benzoate **51h** in 89% yield; ¹H NMR (400 MHz, DMSO-*d*₆) δ 0.51–0.53 (2H, m), 0.68–0.69 (2H, m), 1.54–1.58 (5H, m), 1.69–1.74 (2H, m), 1.84–1.87 (6H, m), 1.92–2.08 (4H, m), 4.03–4.09 (1H, m), 7.44 (1H, d, *J* = 7.1 Hz), 7.62–7.68 (2H, m), 8.06 (1H, s), 8.07–8.12 (2H, m), 13.16 (1H, s); HRMS (EI) for C₂₅H₃₀O₃N₃ (MH⁺); calcd, 420.2282; found, 420.2281.

4-[4-(2-Adamantylcarbamoyl)-5-tert-butyl-pyrazol-1-yl]-benzoic Acid (27). 2 M aqueous sodium hydroxide solution (51.7 mL, 103.32 mmol) was added to methyl 4-[4-(2-adamantylcarbamoyl)-5-tert-butyl-pyrazol-1-yl]benzoate **51a** (4.5 g, 10.33 mmol) in methanol (100 mL). The mixture was stirred at 70 °C for 1 h and then cooled to ambient temperature, concentrated under reduced pressure and diluted with water (100 mL). The reaction mixture was adjusted to pH 3 with 2 M HCl. The reaction mixture was extracted with EtOAc (500 mL) and washed sequentially with water (2 \times 100 mL), and saturated brine (50 mL). The organic layer was dried over MgSO₄, filtered and evaporated to give a pale yellow solid. The solid was washed with EtOAc (20 mL), collected by filtration and dried under vacuum to give a cream crystalline solid (3.89 g, 89%); mp 310–312 °C; ¹H NMR (400 MHz, DMSO-*d*₆) δ 1.18 (9H, s), 1.44–1.54 (2H, m), 1.65–1.87 (8H, m), 1.90–1.92 (2H, m), 2.03–2.12 (2H, m), 3.97–4.01 (1H, m), 7.48–7.51 (2H, m), 7.60 (1H, s), 8.05–8.08 (2H, m), 8.12 (1H, d, *J* = 7.2 Hz), 13.23 (1H, s); HRMS (EI) for C₂₅H₃₂O₃N₃ (MH⁺); calcd, 422.2438; found, 422.2437.

***N*-(2-Adamantyl)-4,4-dimethyl-3-oxo-pentanamide (49a).** A 1 M solution of lithium bis(trimethylsilyl)amide in THF (22.84 mL, 22.84 mmol) was added to THF (25 mL) and cooled under nitrogen to –78 °C. A solution of 3,3-dimethyl-2-butanone (2.287 g, 22.84 mmol) in THF (25 mL) was added dropwise over a period of 5 min. The resulting solution was stirred at –78 °C under nitrogen for 15 min. A solution of 2-isocyanatoadamantane (prepared from 2-adamantylamine hydrochloride by the method of R. Reck and C. Jochims¹⁸) (3.68 g, 20.76 mmol) in THF (20 mL) was added over a period of 5 min. The resulting solution was stirred at –78 °C for 1 h and then allowed to warm to 20 °C over 1 h. The reaction mixture was poured into saturated NH₄Cl (150 mL) and extracted with EtOAc (2 \times 100 mL), the organic layer was washed with water (50 mL) and brine (50 mL) dried over MgSO₄, filtered and evaporated to afford a yellow oil. The crude product was purified by flash silica chromatography, elution gradient 0 to 50% EtOAc in isohexane to afford a white solid (4.64 g, 81%); ¹H NMR (400 MHz, DMSO-*d*₆) δ 1.08–1.09 (9H, m), 1.50 (2H, d), 1.66–1.89 (10H, m), 1.95–2.00 (2H, m), 3.53 (1.4H, s),

3.80–3.94 (1H, m), 5.30 (0.3H, s), 7.77–7.87 (1H, m), 14.43 (0.3H, s) (2:1 mixture of keto and enol forms); LRMS m/z ($M^+ + H$) = 278.

(2)-N-(2-Adamantyl)-2-(dimethylaminomethylidene)-4,4-dimethyl-3-oxo-pentanamide (50a). *N,N*-Dimethylformamide dimethyl acetal (3.02 mL, 22.71 mmol) was added to a stirred suspension of *N*-(2-adamantyl)-4,4-dimethyl-3-oxo-pentanamide **49a** (5.25 g, 18.93 mmol) in 1,4-dioxane (50 mL) under nitrogen. The resulting mixture was stirred at 100 °C for 2 h. The reaction mixture was evaporated to dryness and the resulting pale cream solid was dried under vacuum to afford the title compound (5.83 g, 93%); $^1\text{H NMR}$ (400 MHz, DMSO- d_6) δ 1.13 (9H, s), 1.47 (2H, d), 1.69–1.83 (10H, m), 2.03 (2H, d), 2.92 (6H, s), 3.90 (1H, d), 7.24 (1H, s), 7.94 (1H, d); LRMS m/z ($M^+ + H$) = 333.

Methyl 4-[4-(2-Adamantylcarbamoyl)-5-tert-butyl-pyrazol-1-yl]benzoate (51a). 2-(4-(Methoxycarbonyl)phenyl)hydrazinium chloride (3.04 g, 15.00 mmol) was added in one portion to (2)-*N*-(2-adamantyl)-2-(dimethylaminomethylidene)-4,4-dimethyl-3-oxo-pentanamide **50a** (4.99 g, 15 mmol) in ethanol (100 mL). Five drops of acetic acid were added and the resulting solution was stirred at 80 °C for 2 h. The reaction mixture was concentrated and diluted with EtOAc (500 mL), and washed sequentially with water (200 mL), and saturated brine (200 mL). The organic layer was dried over MgSO_4 , filtered and evaporated to afford crude product that was purified by flash silica chromatography, elution gradient 0 to 50% EtOAc in isohexane. Pure fractions were evaporated to dryness to afford title compound (4.66 g, 71%) as a yellow solid; $^1\text{H NMR}$ (400 MHz, DMSO- d_6) δ 1.19 (9H, s), 1.50 (2H, d), 1.69–1.95 (10H, m), 2.09 (2H, d), 3.91 (3H, s), 3.99 (1H, d), 7.53–7.56 (2H, m), 7.62 (1H, s), 8.09–8.12 (2H, m), 8.20 (1H, d); LRMS m/z ($M^+ + H$) = 436.

Log $D_{7.4}$. Measurements were made using a shake-flask method where the extent of partitioning between pH 7.4 buffer and octanol was measured.¹⁹ Compounds were dissolved in a known volume buffer, and following the addition of a known amount of octanol, the solutions were shaken for 30 min. Following centrifugation, analysis of the aqueous layer was performed by LC–UV to quantify the amount of compound in solution and then compared to analysis of the compound in solution before the addition of octanol to calculate the partitioning coefficient, $D_{7.4}$.

11 β -HSD1 Activity in Liver and Adipose Tissue. Han Wistar rats were maintained on a chow diet were dosed by oral gavage with compound suspended in 0.5% w/v hydroxypropyl methylcellulose, HPMC (4000–15 000 cPs) and 0.1% w/v Tween 80. Animals were euthanased 3 h post dose using a rising concentration of CO_2 at a time postdose as determined by PK. Blood samples were taken via cardiac puncture for compound determination. Activity of the 11 β -HSD1 enzyme in liver and epididymal adipose tissue was measured as the conversion of ^3H -cortisone to ^3H -cortisol. Liver pieces were removed from rats snap frozen and rat adipose tissue was used fresh following termination. Tissues were weighed (approximately 100–200 mg), cut into 2–3 mm³ pieces using scissors and incubated for 10 min (rat liver) or 90 min (rat adipose tissue) in the presence of ^3H -Cortisone (20 nmol/L, 1 $\mu\text{Ci/mL}$, specific activity 1.97GBq/mmol, Perkin-Elmer) containing DMEM Ham F12 media (Sigma Aldrich, Poole, UK) supplemented with 10% FCS and 1% penicillin–streptomycin (Sigma Aldrich, Poole, UK) in 37 °C at 5% CO_2 . After tissue incubations, medium samples were collected for analysis of ^3H -cortisone to ^3H -cortisol conversion. Radio-labeled steroids were extracted using ethyl acetate, samples were evaporated to dryness under nitrogen and resuspended in mobile phase for HPLC analysis (methanol/ H_2O , 50:50), adapted from Napolitano et al.²⁰ Radiolabeled steroids were separated using reversed phase HPLC, Agilent 1200 HPLC using a Kromasil C18 5 μm column, 4.6 mm \times 250 mm (Crawford Scientific, Lanarkshire, UK) with methanol/ H_2O (50:50) at flow rate of 1.5 mL/min. Radioactivity measured using a flow scintillation analyzer (Radiomatic series 500TR, Perkin-Elmer Analytical Instruments) with FLO-ONE software.

■ ASSOCIATED CONTENT

§ Supporting Information

Experimental details for the syntheses of compounds **5–7**, **10**, **12–17** and intermediates are described together with biological, analytical and crystallographic information. This material is available free of charge via the Internet at <http://pubs.acs.org>.

■ AUTHOR INFORMATION

Corresponding Author

*Tel: +44 (0)1625 232567. Fax: +44 (0)1625 516667. E-mail: jamie.scott@astrazeneca.com.

Notes

The authors declare no competing financial interest.

■ ACKNOWLEDGMENTS

William McCoull is thanked for initial work leading to the identification of the pyrazole scaffold. Gemma Convey, Clare Stacey, Ruth Brownlie and Julie Cook are thanked for the generation of biological data. Peter Barton, Stuart Bennett, Linda Godfrey and John Reville are thanked for synthetic chemistry contributions. Paul Davey is thanked for analytical support.

■ ABBREVIATIONS USED

11 β -HSD1, 11 β -hydroxysteroid dehydrogenase type 1; 11 β -HSD2, 11 β -hydroxysteroid dehydrogenase type 2; Clp, plasma clearance; CYP, cytochrome P450; DMPK, drug metabolism and pharmacokinetics; EDCl, 1-(3-dimethylaminopropyl)-3-ethylcarbodiimide; HMDS, hexamethyldisilazide; HOBT, *N*-hydroxybenzotriazole; LLE, ligand-lipophilicity efficiency; MAP, monophasic action potential; MDCK, Madin-Darby canine kidney cell line; NAD, nicotinamide adenine dinucleotide; NADPH, nicotinamide adenine dinucleotide phosphate; PPB, plasma protein binding; SAR, structure activity relationship; TFA, trifluoroacetic acid

■ REFERENCES

- (1) Grundy, S. M.; Brewer, H. B.; Cleeman, J. I.; Smith, S. C.; Lenfant, C. Definition of metabolic syndrome. *Circulation* **2004**, *109*, 433–438.
- (2) Björntorp, P.; Rosmond, R. Obesity and cortisol. *Nutrition* **2000**, *16*, 924–936.
- (3) Björntorp, P.; Holm, G.; Rosmond, R. Hypothalamic arousal, insulin resistance and Type 2 diabetes mellitus. *Diabetic Med.* **1999**, *16*, 373–383.
- (4) Walker, B. R. Glucocorticoids and Cardiovascular Disease. *Eur. J. Endocrinol.* **2007**, *157*, 545–559.
- (5) Edwards, C. R. W.; Benediktsson, R.; Lindsay, R. S.; Seckl, J. R. 11 β -Hydroxysteroid dehydrogenases: Key enzymes in determining tissue-specific glucocorticoid effects. *Steroids* **1996**, *61*, 263–269.
- (6) Tomlinson, J. W.; Walker, E. A.; Bujalska, I. J.; Draper, N.; Lavery, G. G.; Cooper, M. S.; Hewison, M.; Stewart, P. M. 11 β -Hydroxysteroid dehydrogenase type 1: A tissue-specific regulator of glucocorticoid response. *Endocr. Rev.* **2004**, *25*, 831–866.
- (7) Thieringer, R.; Hermanowski-Vosatka, A. Inhibition of 11 β -HSD1 as a novel treatment for the metabolic syndrome: do glucocorticoids play a role? *Expert Rev. Cardiovasc. Ther.* **2005**, *3*, 911–924.
- (8) Wamil, M.; Seckl, J. R. Inhibition of 11 β -hydroxysteroid dehydrogenase type 1 as a promising therapeutic target. *Drug Discov. Today* **2007**, *12*, S04–S20.
- (9) Webster, S. P.; Pallin, T. D. 11 β -Hydroxysteroid dehydrogenase type 1 inhibitors as therapeutic agents. *Expert Opin. Ther. Patents* **2007**, *17*, 1407–1422.
- (10) Boyle, C. D.; Kowalski, T. J. 11 β -hydroxysteroid dehydrogenase type 1 inhibitors: a review of recent patents. *Expert Opin. Ther. Patents* **2009**, *19*, 801–825.

(11) Morgan, S. A.; Tomlinson, J. W. 11β -Hydroxysteroid dehydrogenase type 1 inhibitors for the treatment of type 2 diabetes. *Expert Opin. Investig. Drugs* **2010**, *19*, 1067–1076.

(12) Wilson, R. C.; Dave-Sharma, S.; Wei, J.; Obeyesekere, V. R.; Li, K.; Ferrari, P.; Krozowski, Z. S.; Shackleton, C. H. L.; Bradlow, L.; Wiens, T.; New, M. I. A genetic defect resulting in mild low-renin hypertension. *Proc. Natl. Acad. Sci.* **1998**, *95*, 10200–10205.

(13) Kotelevtsev, Y.; Brown, R. W.; Fleming, S.; Kenyon, C.; Edwards, C. R. W.; Seckl, J. R.; Mullins, J. J. Hypertension in mice lacking 11β -hydroxysteroid dehydrogenase type 2. *J. Clin. Invest.* **1999**, *103*, 683–689.

(14) Scott, J. S.; Bowker, S. S.; deSchoolmeester, J.; Gerhardt, S.; Hargreaves, D.; Kilgour, E.; Lloyd, A.; Mayers, R. M.; McCoull, W.; Newcombe, N. J.; Ogg, D.; Packer, M. J.; Rees, A.; Reville, J.; Schofield, P.; Selmi, N.; Swales, J. G.; Whittamore, P. R. O. Discovery of a Potent, Selective and Orally Bioavailable Acidic 11β -Hydroxysteroid Dehydrogenase Type 1 (11β -HSD1) Inhibitor: The Discovery of 2-[(3S)-1-[5-(cyclohexylcarbamoyl)-6-propylsulfanyl-pyridin-2-yl]-3-piperidyl]-acetic acid (AZD4017). *J. Med. Chem.* **2012**, *55* (11), 5951–5964.

(15) Stachulski, A. V.; Harding, J. R.; Lindon, J. C.; Maggs, J. L.; Park, B. K.; Wilson, I. D. Acyl Glucuronides: Biological Activity, Chemical Reactivity, and Chemical Synthesis. *J. Med. Chem.* **2006**, *49*, 6931–6945.

(16) Regan, S. L.; Maggs, J. L.; Hammond, T. G.; Lambert, C.; Williams, D. P.; Park, B. K. Acyl glucuronides: the good, the bad and the ugly. *Biopharm. Drug Dispos.* **2010**, *31*, 367–395.

(17) Leeson, P. D.; Springthorpe, B. The influence of drug-like concepts on decision-making in medicinal chemistry. *Nat. Drug Discov.* **2007**, *6*, 881–890.

(18) Reck, R.; Jochims, C. α -Bromisocyanate. *Chem. Ber.* **1982**, *115*, 860–870.

(19) $\log D_{7.4}$, plasma-protein binding and solubility measurements were made as described in: Buttar, D.; Colclough, N.; Gerhardt, S.; MacFaul, P. A.; Phillips, S. D.; Plowright, A.; Whittamore, P.; Tam, K.; Maskos, K.; Steinbacher, S.; Steuber, H. A. Combined spectroscopic and crystallographic approach to probing drug–human serum albumin interactions. *Bioorg. Med. Chem.* **2010**, *18*, 7486–7496.

(20) Napolitano, A.; Voice, M. W.; Edwards, C. R. W.; Seckl, J. R.; Chapman, K. E. 11β -hydroxysteroid dehydrogenase 1 in adipocytes: Expression is differentiation-dependent and hormonally regulated. *J. Steroid Biochem. Mol. Biol.* **1998**, *64*, 251–260.